AN EXPERIMENTAL TEST BENCH FOR THE THERMAL CONDITIONING ANALYSIS OF ABSORPTION AND DESORPTION CYCLES OF HYDROGEN WITHIN METAL HYDRIDES STORAGE TANKS

Riccardo Alleori[1], Maria Alessandra Ancona[2], Michele Bianchi[2], Francesco Falcetelli[2], Federico Ferrari[2]*, Paolo Pilati[3]

[1] Alma Mater Studiorum Università di Bologna, Inter-Departmental Center for Industrial Research on Renewable Sources, Environment, Sea and Energy (CIRI-FRAME), Via Terracini 24, 40131 Bologna, Italy
[2] Alma Mater Studiorum Università di Bologna, Department of Industrial Engineering (DIN), Viale del Risorgimento 2, 40136 Bologna, Italy
[3] Alma Mater Studiorum Università di Bologna, Department of Electrical, Electronic and Information Engineering (DEI), Viale del Risorgimento 2, 40136 Bologna, Italy

* Corresponding Author: federico.ferrari28@unibo.it

ABSTRACT

Hydrogen storage is one of the key issues to its spread on a large scale; among the different methods, storing hydrogen in the form of metal hydrides is certainly a promising technology due to several aspects, including the lack of hydrogen compression. However, this process is not mature yet and further studies are needed to make this storage system competitive; in particular, due to thermal behavior of metal hydrides during the absorption/desorption phases, the heat management of the storage system needs to be improved, to enhance the reaction kinetics in the metal site.
This work aims at presenting an experimental test bench, built to characterize and optimize the thermal conditioning and management of low-pressure metal hydrides canisters for hydrogen storage, fed by a green hydrogen production line. More in detail, the final objective of this scientific path is to propose an experimental approach for the energy assessment of the hydrogen storage system in metal hydrides, no longer in an isolated way but in the perspective of integration with the commercial electrolysis technology for stationary applications. This approach will therefore allow a necessary overview to experimentally investigate the effects of the metal hydrides thermodynamic behaviour on the entire Power-to-Hydrogen system, allowing to define a methodology for the optimized integration between systems by means of some empirical correlations, to increase energy efficiency and reduce operating costs/risks.

1 INTRODUCTION

Hydrogen as an energy carrier could be a new additional strategy to decarbonize the energy sector. It can be produced by electrolysis starting from the surplus power of renewable sources and then it can be stored and reconverted into electricity, when needed, by means of fuel cells, without pollutant emissions. In the context of energy transition from fossil fuels to renewable and more sustainable sources, hydrogen is therefore recognized as a potential environmentally friendly energy vector, although – due to its physical nature – its storage presents itself as a major challenge for the spread of the hydrogen economy on a large scale (Usman *et al*., 2022). Hydrogen storage can be approached through different physical and chemical methods (i.e., compressed, liquefied, involved in nanostructured and solid-state materials), each exhibiting specific advantages and drawbacks. In the last decade, a significant effort has been made to develop novel storage technologies, such as Metal Hydrides (MH), which are considered among the most promising technologies in the hydrogen industry. Under the proper temperature and pressure conditions, metal hydrides can absorb and desorb hydrogen

https://doi.org/10.52202/077185-0097

in a reversible way and this property makes them particularly attractive from the perspective of a sustainable clean energy transition (Pasquini *et al*., 2022). Moreover, their relatively low working pressure could imply a more efficient and safer storage solution for Power-to-Gas (P2G) and Power-to-Power (P2P) applications, ensuring a compact storage system with the possibility of increasing the overall plant efficiency by recovering waste heat from fuel cells operation to be used for hydrogen desorption (Tarasov *et al*., 2021).

Nevertheless, the transition of metal hydride technology from a prototype scale to industry requires further efforts by academic and industrial research, to achieve greater knowledge in terms of material properties and reaction kinetics (Rusman *et al*., 2016). Indeed, from the thermodynamic point of view, the thermal behavior of MH during the absorption and desorption cycles could be difficult to predict: especially when moving from the specimen level toward the real system scale, additional factors (such as the shape of the shell and the hydrogen supply points positioning) must be considered (Suàrez *et al*., 2022, Askri *et al*., 2009). Moreover, operating close to the minimum or maximum allowed temperature may cause the degradation of the metallic powder and therefore of the storage capacity. In these circumstances, special maintenance procedures are required for the reconditioning of the metallic compound inside the canister, which are both cost- and time-consuming (Sakintuna *et al*., 2007).

In this scenario, this paper is aimed at presenting the first important results – obtained by the University of Bologna – in the context of the NoMaH (Novel Materials for Hydrogen storage) project (*NoMaH* website), funded by European Union - NextGenerationEU - PNRR (Italian National Recovery and Resilience plan). The project is focused on the fundamental research and development of innovative hybrid solutions for hydrogen storage, intended for energy communities and production districts, by the exploitation of complementary storage technologies such as cryo-adsorption, organic and intermetallic compounds, nanostructured metal hydrides and, for higher capacity solutions, ammonia, with the final purpose of realize a hybrid storage system demonstrator. The project is carried out by the University of Bologna (UniBo) in collaboration with University of Calabria (UniCal - project leader), Polytechnic University of Torino (PoliTo), Polytechnic University of Bari (PoliBa) and Rina Consulting Centro Sviluppo Materiali S.p.A. (RINA-CSM).

In particular, the aim of this study is to present the P2G test bench built up by the Machines and Energy Systems Research Group of the University of Bologna to develop and test optimization strategies for the thermal management of metal hydrides canisters for hydrogen storage, with the final goal to propose a methodology for the systems integration and sizing between low-pressure/temperature metal hydrides and electrolysis technology for Power-to-Hydrogen systems.

2 METHODOLOGY

2.1 Fundamentals of metal hydrides physics

Many transition metals, when exposed to hydrogen in gaseous form, can bind to it forming interstitial binary hydrides. Interstitial hydrides can consist of alloys of one or more elements, of which the first, A, characterized by the main property of easily bind to hydrogen, while the second, B, has the function of limit and control the affinity of interaction of the first element with hydrogen. The common classification of intermetallic compounds for hydrogen divides them into AB, AB2, AB5 and A2B, such as TiFe, TiCr2, LaNi5 and Mg2Ni.

The process of hydrogen absorption by the metal, or hydrogenation, can be thermodynamically described by isotherm curves in a pressure-composition graph, as shown in Fig. 1 (Klopčič *et al.*, 2023). At fixed temperature, the molecular hydrogen, put in contact with the metal, initially interacts with its surface through weak electrostatic forces (Van der Waals). Subsequently, due to the metal collisions, it dissociates into hydrogen atoms, which – thanks to the small size – begins then to spread inside the lattice, occupying the empty positions (called interstitial sites). By gradually supplying hydrogen to the system at a greater pressure than the threshold value, a phase, in which the maximum concentration of hydrogen within the interstitial sites can be obtained, while maintaining the pressure almost constant ($\alpha + \beta$), is reached. At this stage, therefore, the so-called "plateau" of the pressure-composition curve is observed. At last, by still injecting hydrogen, there is a rapid increase in pressure with the concentration (β phase).

https://doi.org/10.52202/077185-0097

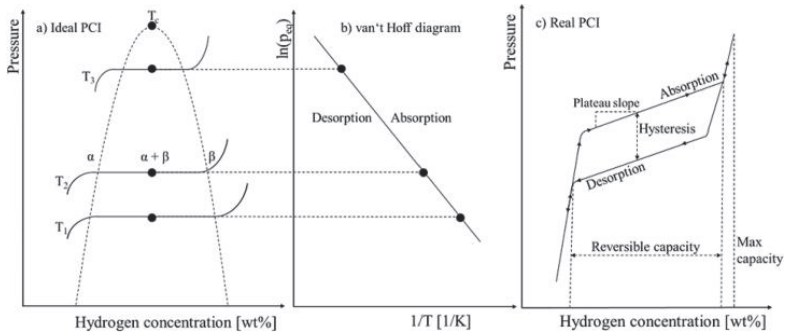

Figure 1: Example of ideal (left) and real (right) Pressure-Composition-Isotherm (PCI) curves and Van't Hoff diagram (center) for MH intermetallic compounds, highlighting the three regions α, α + β and β (Klopčič *et al.*, 2023).

2.2 Test bench description

The proposed system layout is shown in Fig. 2: it consists of a hydrogen line composed of two alternative charging and one discharging branches, combined with a thermal conditioning section for the MH storage system. The preliminary results of the experimental campaign reported in this work are referred to the charging section of the plant, with the aim to investigate the coupling between the PEM electrolyzer and the MH storage system. Future works will focus more extensively both on the high-pressure charging section and on the discharging process by means of the PEM fuel cell.

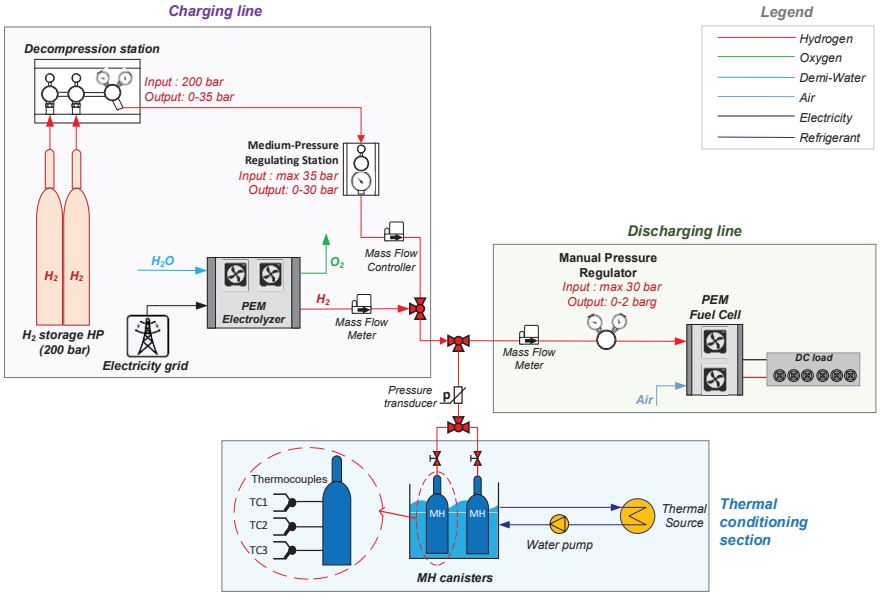

Figure 2: Layout of the final MH-based P2G test bench, consisting of separate charging and discharging branches and of a thermal conditioning section.

The first charging line is powered by an external high-pressure reservoir (200 bar), while the second one is linked to a Proton Exchange Membrane (PEM) electrolyzer. In more detail, the current experimental set-up is composed of:

i) a PEM electrolyzer, able to produce 2.46 g/h (27.59 NL/h) of hydrogen at 10.5 bar, with a nominal power consumption of 300 W (AC) – Fig. 3*a*;
ii) a hydrogen storage system, namely three metal hydride canisters of 16.9 g (189.6 NL) each one able to store hydrogen at a maximum pressure of 10 bar – Fig. 3*b*;

https://doi.org/10.52202/077185-0097

iii) a water-cooling circuit as thermal conditioning system for the MH canisters consisting of a centrifugal water pump, a thermal buffer tank and a self-built water-bath heat-exchanger – Fig. 3*c* and Fig. 3*d*;
iv) a data acquisition system realized in LabVIEW™ environment and based on National Instruments™ instrumentation. In detail, 8-slot chassis NI-DAQ 9133 is installed, equipped with:
• two NI-9211 input modules for thermocouples;
• one NI-9203 input module for analog current signals (0 ÷ 20 mA);
• one NI-9201 module for analog voltage signals (0 ÷ 10 V).

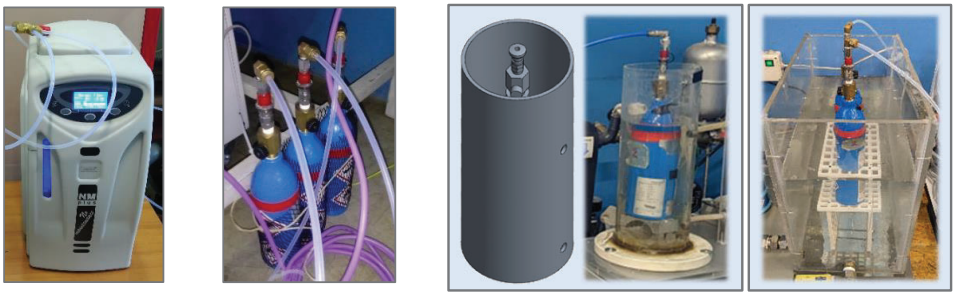

a) *b*) *c*) *d*)

Figure 3: *a*) PEM Hydrogen generator; *b*) MH canisters; *c*) first and *d*) final prototypes of the water-bath heat-exchangers of the thermal conditioning system.

A comprehensive overview of the experimental test-bench in its actual configuration is given in Fig. 4.

Figure 4: Overview of the current experimental setup.

Further technical specifications on the electrolyzer and the MH canisters are reported below in Table 1 and Table 2, respectively.
As regards the DAQ station, it has been equipped with several transducers and sensors to monitor the main thermodynamic quantities (such as pressures, flow rates and temperatures), as shown in the conceptual scheme of Fig. 2. Furthermore, a summary table of the measurement points on the plant is given in Table 3.

Table 1: Hydrogen generator technical specifications (*Heliocentris, 2015)*

Property	Value
Type	PEM
Hydrogen flow rate	2.46 g/h (27.59 NL/h)
Max. outlet pressure	10.5 bar (155 psi)

https://doi.org/10.52202/077185-0097

Hydrogen purity	6.0 (99.9999%)
Power consumption	300 VA
Input voltage	110-230V / 50-60 Hz
Operating conditions	
Temperature	+15 °C ÷ +40 °C
Relative humidity	0÷80%

Table 2: MH canisters technical specifications (*Heliocentris, 2015)*

Property	**Value**
Type	AB_2
Capacity	16.9 g (189.6 NL) (each)
Hydrogen purity	5.0 (99.9999%)
Max. permissible pressure	10 bar
Operating temperature (discharging /filling)	–5 °C ÷ +55 °C
Ambient temperature (during operation)	+5 °C ÷ +30 °C
Absorption	
Charging pressure	10 bar @ +20°C
Recommended starting temperature	< 30 °C
Desorption	
Recommended desorption rate	1.42 NL/min
Recommended starting temperature	> 5 °C
Diameter	70 mm
Length | Weight | Volume	309 mm | 2.2 kg | 0.5 L

Table 3: Investigated physical quantities and corresponding sensors installed in the test bench.

Physical quantity	**Symbol**	**Unit**	**Sensor**	**Accuracy**	**Measuring range**	**Output signal**
H_2 delivery pressure (to canisters)	$p_{H2,del}$	bar	Pressure transducer	± 0.25 FS	0 ÷ 15 bar	0 ÷ 10 V
H_2 delivery mass flow	$\dot{m}_{H2,del}$	NL/min	Thermal mass flow meter	± 0.5 % FS	0.1 ÷ 85 NL/min	4 ÷ 20 mA
Ambient temperature	T_{amb}	°C	T-type thermocouple	± 0.5 °C	–20 ÷ 350 °C	TC
Heat-exchanger chamber water temperature	$T_{water\text{-}HX}$	°C	T-type thermocouple	± 0.5 °C	–20 ÷ 350 °C	TC
Surface canister temperature (top)	T_{top}	°C	K-type thermocouple	± 0.5 °C	–75 ÷ 250 °C	TC
Surface canister temperature (middle)	T_{middle}	°C	K-type thermocouple	± 0.5 °C	–75 ÷ 250 °C	TC
Surface canister temperature (bottom)	T_{bottom}	°C	K-type thermocouple	± 0.5 °C	–75 ÷ 250 °C	TC
Mechanical strain	ε	µm/m	Optical fiber sensor	± 1 µm/m	0 ÷ 4000 µm/m	Digital

Specifically, the temperature on each canister has been measured employing three K-type thermocouples positioned at three different locations (bottom, middle and top). This configuration allows to map any temperature gradients caused by the canister internal geometry and non-uniform absorption/desorption dynamics. The thermocouple locations were chosen after a preliminary qualitative analysis made with a thermal imaging camera (see Fig. 5).

https://doi.org/10.52202/077185-0097

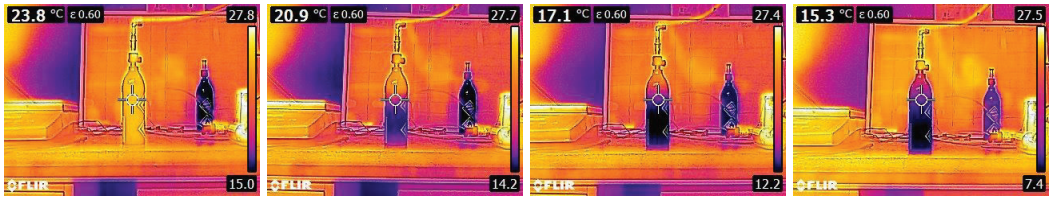

Figure 5: Sequence of qualitative images taken by infrared thermal camera to monitor the surface temperature field during a hydrogen desorption test (left to right).

2.3 Experimental design

Thermodynamic analysis - The experimental characterization of the MH storage during the absorption phase can be carried out in two different ways.

The first is focused on the behavior of the coupling between a PEM electrolyzer and MH as hydrogen storage system: the absorption phase is managed by a commercial PEM hydrogen generator, which produces and releases hydrogen with its own control logic, based on the pressure difference between the production set-point value and the delivery one. This set-up results in a variable hydrogen flow rate profile depending on the downstream thermodynamic conditions (*pressure driven mode)*.

The second test mode is performed by means of the hydrogen line, starting from the high-pressure external reservoir, and involves a control on the flow of hydrogen entering the canisters in order to map the system performance throughout its operating range under different boundary conditions (i.e., hydrogen flow rate, ambient and conditioning temperature, charging/discharging pressure). More in detail, the isolated characterization of MH starts with the decompression station which reduces the hydrogen pressure from the external 200 bar storage to the value of 35 bar, before being further decreased by a second reduction stage to the delivery value, in any case within 30 bar. Downstream of the second reduction stage, a mass flow controller is installed, allowing the complete control of the hydrogen mass flow rate delivered to the canisters *(flow rate driven mode)*.

In this work only the first experimental set-up is considered. Therefore, the aim of the investigation moves towards the thermal behavior of MH cylinders coherently with the variable hydrogen production profile from the electrolyzer, as a result of its operating conditions and of the availability of surplus power from RES. In this arrangement it is possible to act only on the filling pressure value, while the hydrogen flow is regulated by the electrolyzer. The thermal response of the cylinders can therefore be considered a macroscopic indicator of how the chemical kinetics of metal hydrides formation will follow the continuous equilibrium pressure shift, due to the fluctuations of the hydrogen production profile.

As mentioned above, temperature is a physical parameter that plays a key role during the charging and discharging phases, due to the respectively exothermic and endothermic behavior of the involved chemical reactions. For these reasons, during the absorption process the canisters need to be cooled: a thermal conditioning system circuit, consisting of a prototypal heat exchanger, a pump and a cold thermal source, allows to immerse the canisters in a water-bath – Fig. 6.

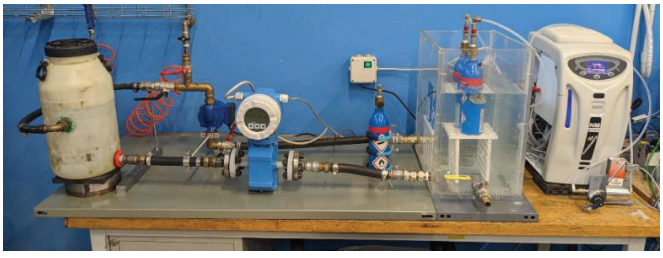

Figure 6: detailed view of the thermal conditioning system in its final configuration.

The same experimental approach is adopted for the desorption phase, during which the canisters are heated within the thermal conditioning circuit while the hydrogen flow is deflected by a three-way valve

https://doi.org/10.52202/077185-0097

towards a PEM fuel cell, fed with a hydrogen pressure of 0.55 barg. An interesting improvement on the test-bench could be represented by the adoption of a secondary heat exchanger to be implemented on the fuel cell for thermal power recovery in order to pre-heat the canisters and enhance the overall system efficiency.

Monitoring of mechanical strain - The experimental investigation comprehends also the mechanical strain arising from the adsorption/desorption cycles. Indeed, from a mechanical perspective the adsorption/desorption cycles produce a cyclic fatigue load on the canister structure. Therefore, to ensure an adequate level of safety of the storage system it is of utmost importance to develop an appropriate strain monitoring system. This aspect of the research aims at enabling the remaining useful life estimation of the storage system and providing guidance on the possible maintenance strategies.

Non-contact solutions such as Digital Image Correlation (DIC) offer the opportunity to monitor the bidimensional strain field. However, the presence of the thermal conditioning system around the canister and the presence of turbulent water limits the use of this technology and other non-contact approaches. Conventional strain gauges can be a solution, but they require high-level expertise in the installation phase, surface treatment of the canister (which is not always feasible). Moreover, special care must be taken to compensate temperature variations which are responsible of modifying the gauge factor and producing apparent strain readings due to the difference between the temperature expansion coefficient of the grid and the substrate material.

In this scenario Optical Fiber Sensors (OFSs) seems to be the most effective solution for strain monitoring. First, OFSs are intrinsically immune from electromagnetic interference contrary to common electrical strain gauges. Their passive nature makes them perfect candidates for monitoring solutions where potential sparks might lead to catastrophic failures. Moreover, OFSs have excellent durability records and a relatively easy installation procedure. Fiber Bragg Gratings (FBG) sensors have one the highest technology readiness level among the OFSs landscape and show extremely high multiplexing capabilities, which are particularly useful when measuring multiple point simultaneously.

Figure 7: FBG sensor setup and data acquisition system.

According to the FBG sensing principle, both strain, ε, and temperature variations, ΔT, cause a variation of the Bragg's wavelength, λ_B, according to the following equation:

$$\frac{\Delta\lambda_B}{\lambda_B} = K_\varepsilon \varepsilon + K_T \Delta T \quad (1)$$

where K_ε and K_T represent the coefficients linking the changes of the Bragg's wavelength with strain and temperature variations, respectively.

In this specific application, the aim is to measure only the mechanical strains arising from the adsorption/desorption cycles. Indeed, thermal induced strains are not relevant from a mechanical point of view since they manifest themselves without any load on the structure. Despite the presence of the thermal conditioning system, the canister is undergoing unavoidable temperature variations, therefore, the second term of equation 1 cannot be neglected. The ΔT value can be obtained from the TC2 thermocouple that is in the proximity of the FBG sensor (see Fig. 7).

To obtain the strain value associated with a certain $\Delta\lambda_B$, it is necessary to compensate for the apparent strain reading arising from the second term of equation 1, which can be described as follows:

$$K_T \Delta T = (CTE + \eta)\, \Delta T \quad (2)$$

https://doi.org/10.52202/077185-0097

where CTE and η represent the coefficient of thermal expansion (CTE) for the fiber and the thermo-optic coefficient (η), respectively. In loose conditions, thermal expansion coefficient for the silica fiber would be equal to approximately $\mathrm{CTE} \cong 0.55 \cdot 10^{-6}\ °C^{-1}$. On the other hand, assuming a perfect bonding of the FBG sensor on the canister surface and, thus, an ideal strain transfer from the substrate to the core of the FBG sensor, the thermal expansion of FBG sensor matches the thermal expansion of the steel canister since the latter is significantly stiffer compared to silica (i.e., $\mathrm{CTE} = \mathrm{CTE}_{\mathrm{Al-Bronze}} \cong 20 \cdot 10^{-6}\ °C^{-1}$). Finally, the thermo-optic effect must be considered. For a germanium-doped silica optical fiber, η can be considered approximately equal to $8.6 \cdot 10^{-6}\ °C^{-1}$ (Othonos *et al.*, 2006).
In the next section are presented the preliminary results of the first experimental investigation, focused on the PEM – MH plant configuration.

3 RESULTS

3.1 Absorption and desorption analysis

The preliminary experimental investigations allowed to map over time the surface thermal profile for each canister at different coolant temperatures. As mentioned above, both the tests that will be shown are based on the PEM-E – MH coupling during the charging phase but two different thermal management set-ups with different boundary conditions were considered: the first configuration involves a canister not thermally conditioned (free convection in ambient air), while the second test has been done by immersing the canister in a water-ice bath (free convection).
As for the hydrogen production side, both the tests have been done with a control on the set-point pressure within the canisters, with a final value of 10 bar, leaving the electrolyzer free of working in floating mode with full availability of electric input power. To this purpose, for each experimental set-up the absorption cycle starts with the canister at ambient pressure and ends when its internal pressure reaches 10 bar (*pressure driven mode*).
In Fig. 8*a*, it can be observed the trend of the surface temperature in correspondence of the three monitored positions (top, middle and bottom) of the MH canister during an absorption cycle in air, while Fig. 8*b* shows the surface temperature profiles on the same monitored positions during the absorption cycle in water-ice bath: the exothermic nature of the reaction leads to an increase in MH temperature as the reaction goes on. In particular, the region that tends to warm up significantly is the one located in the lowest part of the canister, due to its internal geometry and dispenser disposition. The severe cooling to which the cylinder was subjected (see Fig. 8*b*) led to a slower pressure growth over time during the absorption process, considering the same end-point pressure value of 10 bar (see Fig. 9*a*). Referring to the physical principles explained previously, the better thermal conditions allowed to absorb hydrogen in a more efficient way shifting down the equilibrium pressure in the Pressure-Composition-Isotherm representation.

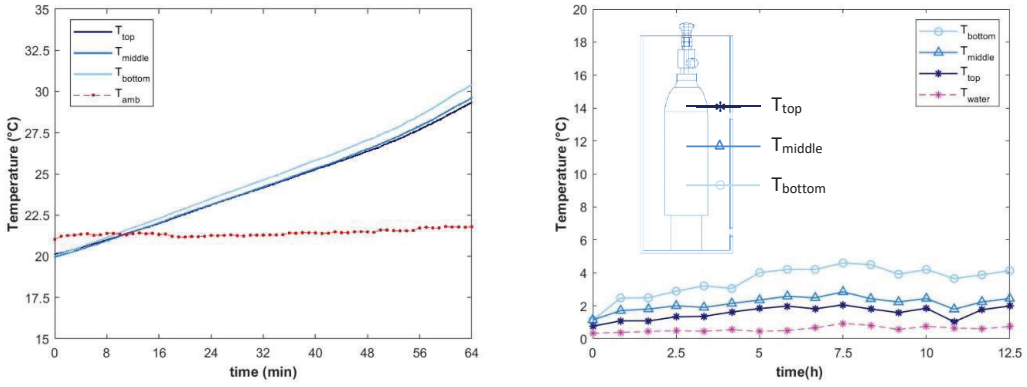

a) *b)*

Figure 8: Surface MH temperatures during absorption in air (*a*) and in water-ice bath (*b*).

https://doi.org/10.52202/077185-0097

It can also be highlighted that despite the more intense thermal conditioning, the canister surface still tends to heat up, marking a noticeable difference between the top and bottom temperatures of the MH canister. This behavior, as a confirmation of what shown also for the previous test, suggests that it might be useful to provide a non-uniform coolant distribution to the canister surface by placing, as an example, the water delivery point in a lower position of the prototypal heat exchanger.
The quantity of hydrogen absorbed by the metal powder is described by the *wt%* index:

$$wt\% = \frac{m_{H2}}{m_{H2}+m_{MH}} \cdot 100 \tag{3}$$

Where m_{H2} represents the mass of absorbed hydrogen [g] and m_{MH} is the weight of the metal powder [g]. However, in this work the log(P)-*wt*% curve, obtained experimentally and shown in Fig. 9*a,* refers to the $wt\%_{SS}$, which is obtained by replacing in Eq. 3 the metal powder mass with the whole storage system mass (m_{SS}), coherently with the system based experimental approach.
As soon as the electrolyzer reaches the set-point working pressure (10 bar), it starts to release hydrogen towards the canister, firstly causing a rapid increase of pressure without, however, accumulating a significant amount of hydrogen. Indeed, in the first part of the charging phase, the mass of hydrogen sent by the electrolyzer exceeds what can be effectively absorbed, thus a share of hydrogen remains unbound to the metal powder, causing an increase of the pressure. Nevertheless, in the next phase the absorption reaction is favored both by the reduced amount of hydrogen sent by the electrolyzer (see Fig. 9*b*) and by the extremely low working temperature.

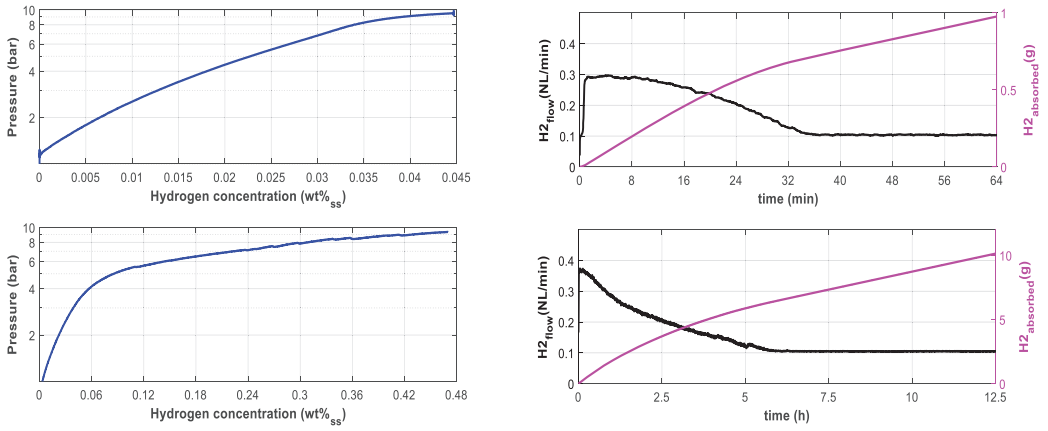

a) *b)*

Figure 9: (*a*) MH pressure as function of the amount of hydrogen stored ($wt\%_{ss}$); (*b*) comparison between flow rate and hydrogen absorbed within MH for both the experimental set-ups.

In the *pressure driven mode*, the hydrogen flow rate sent to the canisters during the tests differs significantly due to the different boundary conditions and the pressure rise within them, as a direct consequence of their thermal management. Specifically, considering the first MH configuration (free convection in ambient air) the PEM electrolyzer started to supply hydrogen with a maximum flow rate slightly above 0.3 NL/min and reached the stable value of 0.1 NL/min after 33 minutes. On the other hand, with the canister immersed in the water-ice bath, the hydrogen flow rate initially reached values of around 0.38 NL/min decreasing after 6 hours to the same stable value of 0.1 NL/min. Ideally, if the pressure remains constant while the $wt\%_{ss}$ increases, the absorption phase reaches its optimal state. As expected, the ideal equilibrium pressure is not achieved, but the trend increases with a much lower slope than the starting phase. Therefore, by keeping the temperature at which the reaction occurs as low as possible, it is possible to control the pressure growth and ensure that what is stored inside the canister

https://doi.org/10.52202/077185-0097

is hydrogen in the form of metal hydrides. On the other hand, implementing such an intense cooling of the canister results in an extended duration of the absorption phase, obtaining approximately 10 g (112 NL) of hydrogen in about 12.5 hours, a significantly higher value compared to 1 g (11.2 NL) stored in the ambient air MH set-up. In particular, the amount of hydrogen stored in the water-cooled system corresponds to an energy per unit of mass of storage equal to 0.151 kWh/kg considering the Lower Heating Value (LHV) of the hydrogen, while if the Higher Heating Value (HHV) is considered, it is approximately 0.180 kWh/kg. Whereas, if the amount of stored energy is referred to a unit of volume, it results respectively in 0.660 kWh/L and 0.788 kWh/L.

3.2 Mechanical stress analysis

The mechanical stress analysis performed with a FBG sensor is shown in Fig. 10. The graph shows the strain trend against time together with temperature (red line with triangular markers) and internal pressure (green line with circle markers) during the first 6 hours of test with the canister in water-ice bath.

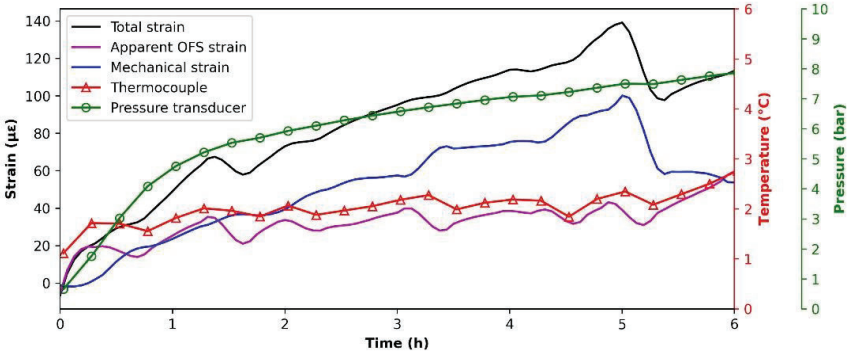

Figure 10: Measured circumferential strains in the MH canister through FBG sensor.

As explained in section 2.3, the FBG measures a strain which can be thought as the sum of the mechanical strain and the apparent strain due to the temperature changes. Therefore, the total strain is the sum of these contributions and is represented in Fig. 10 with the black line. On the other hand, the apparent strain arising by the steel dilatation and thermo-optic coefficient effect in presence of temperature changes is shown by the magenta line. It is interesting to notice that after compensating the temperature effects, the mechanical strains are still present and have an increasing trend, proving the internal volume increment of the MH pushing on the canister internal surface.

4 CONCLUSIONS

This study is intended to present the preliminary results obtained after the first experimental campaign led under the NoMaH project, focused on the thermal conditioning analysis during the hydrogen absorption cycles of a MH storage system. Different configurations have been tested and analyzed, with the aim to compare the cooling effect on the chemical storage system performance. For the thermodynamic analysis, the surface temperatures of each canister have been monitored over time by means of K thermocouple sensors while the surface temperature field has been mapped thanks to a sequence of shots made with an infrared thermal camera. The results show the presence of a significant thermal gradient along the vertical direction of the canisters, even if the test has been performed in ice-water bath conditions within the prototypal heat exchanger. This behaviour could be a direct consequence of the canister internal geometry of the hydrogen distribution channels and should be minimized in future developments by an improved thermal conditioning system, to enhance the absorption/desorption efficiency. To this respect, the flow rate of hydrogen sent to the canisters over the total time of the test, can be intended as a consequence of the MH thermal conditioning on the behaviour of the PEM electrolyzer, and of course of the whole P2G system. In addition, a preliminary

https://doi.org/10.52202/077185-0097

stress analysis show that the canister shell is undergoing moderate strain fatigue cycles due to the volume dilatation phenomena associated with the MH formation. In future developments, further investigations on the mechanical stresses, arising at the canister surface, will be carried out in the perspective of better estimating the remaining useful life of each device.

NOMENCLATURE

A	More hydratable element
AC	Alternate Current
B	Less hydratable element
CTE	Coefficient of Thermal Expansion
DIC	Digital Image Correlation
DAQ	Data Acquisition
FBS	Fiber Bragg Gratings
FS	Full Scale
HG	Hydrogen Generator
HHV	Higher Heating Value
HX	Heat Exchanger
K	Coefficient related to the change of the Bragg's wavelength
LHV	Lower Heating Value
MH	Metal Hydride
NI	National Instruments
NL	Normal Liters
NoMaH	Novel Materials for Hydrogen storage
NTP	Standard Temperature and Pressure (0 °C, 1 atm)
OFSs	Optical Fiber Sensors
P2G	Power-to-Gas
P2P	Power-to-Power
PCI	Pressure Composition Isotherm
PCT	Pressure Concentration Temperature
PCS	Power Conditioning System
PEM	Proton Exchange Membrane
PEM-E	Proton Exchange Membrane Electrolyzer
PNRR	Italian National Recovery And Resilience Plan
RV	Reading Value
STP	Standard Temperature and Pressure (20 °C, 1 bar)
TC	Thermocouple

Symbols

α, $\alpha + \beta$, β	Regions of PCI
ε	Mechanical strain
λ	Wavelength
η	Thermo-optic coefficient

Subscripts

amb	ambient
bottom	bottom of the MH canister
B	Bragg
del	delivery
H2	Hydrogen
middle	middle of the MH canister
SS	Storage System
T	temperature
top	top of the MH canister

https://doi.org/10.52202/077185-0097

ε	Mechanical strain

REFERENCES

Askri, F., Salah, M. B., Jemni, A., Nasrallah, S. B., 2009, Optimization of Hydrogen Storage in Metal-Hydride Tanks, *Int. J. of Hydrogen Energy*, vol. 34, no. 2: p. 897-905.

Heliocentris, solar hydrogen extension mobile unit for solar hydrogen production, http://shecey.com/wp-content/uploads/2015/09/Solar-Hydrogen-Extension_Brochure_EN_1106.pdf.

Klopčič, N., Grimmer, I., Winkler, F., Sartory. M., Trattner, A., 2023, A review on metal hydride materials for hydrogen storage, *J. Energy Storage*, vol. 72, p. 108456.

Othonos, A., Kalli, K., Pureur, D., Mugnier, A. 2006, Fibre Bragg Gratings. In: Venghaus H, editor. *Wavelength Filters in Fibre Optics*. Springer Berlin Heidelberg; p. 189–269.

Pasquini, L. et al., 2022, Magnesium- And Intermetallic Alloys-Based Hydrides for Energy Storage: Modelling, Synthesis and Properties, *Prog. Energy*., vol. 4, no. 3: p. 032007.

Rusman, N. A. A., Dahari, M., 2016, A Review on The Current Progress of Metal Hydrides Material for Solid-State Hydrogen Storage Applications, *Int. J. of Hydrogen Energy*, vol. 41, no.28: p. 12108-12126.

Sakintuna, B., Lamari-Darkrim, F., Hirscher, M., 2007, Metal Hydride Materials for Solid Hydrogen Storage: A Review, *Int. J. of Hydrogen Energy*, vol. 32, no. 9: 1121-1140.

Suarez, S. H., Chabane, D., N'Diaye, A., Ait-Amirat, Y., Djerdir, A., 2022, Static and Dynamic Characterization of Metal Hydride Tanks for Energy Management Applications, *Renewable Energy*, vol. 191, p. 59-70.

Tarasov, B. P. et al., 2021, Metal Hydride Hydrogen Storage and Compression Systems for Energy Storage Technologies, *Int. J. of Hydrogen Energy*, vol. 46, no. 25: p. 13647-13657.

Usman, M. R., 2022, Hydrogen Storage Methods: Review and Current Status, *Renewable and Sustainable Energy Reviews*, vol. 167, p. 112743.

ACKNOWLEDGEMENT

Funded by European Union - NextGenerationEU - PNRR, M2C2.3.5. Views and opinions expressed are however those of the author(s) only and do not necessarily reflect those of the European Union or of the European Commission or of the Italian Ministry of the Environment and Energy Security. Neither the European Union nor the European Commission nor the Italian Ministry of the Environment and Energy Security can be held responsible for them.
The authors would also like to thank the Research Group for industrial applications of plasmas for the use of the FLIR thermal imaging camera.

https://doi.org/10.52202/077185-0097